# Enzymatic Properties of Rat Myelencephalon-Specific Protease †

**ARTICLE** *in* BIOCHEMISTRY · FEBRUARY 2002

Impact Factor: 3.02 · DOI: 10.1021/bi015781a · Source: PubMed

# Enzymatic Properties of Rat Myelencephalon-Specific Protease†

Sachiko I. Blaber,‡ Isobel A. Scarisbrick,§ Matthew J. Bernett,‡,|| Pushparani Dhanarajan,⊥ Margaret A. Seavy,⊥ Yonghao Jin,|| Martin A. Schwartz,|| Moses Rodriguez,§ and Michael Blaber*,‡,||

*Institute of Molecular Biophysics, Department of Chemistry and Biochemistry, and Department of Biological Science, Florida State University, Tallahassee, Florida 32306-4380, and Departments of Neurology and Immunology, Mayo Medical and Graduate School, Mayo Clinic Rochester, Rochester, Minnesota 55905*

*Received September 19, 2001; Revised Manuscript Received November 20, 2001*

ABSTRACT: Myelencephalon-specific protease (MSP), first identified in the rat and now known to have a human homologue (human kallikrein 6), is preferentially expressed in the central nervous system (CNS), compared with nonneural tissues. MSP has been postulated to have trypsin-like activity, is upregulated in response to glutamate receptor-mediated excitotoxic injury in the CNS, and is downregulated in the brain of Alzheimer's patients. The preferential expression of this enzyme by oligodendrocytes in CNS white matter points to a role in myelin homeostasis. To further characterize the activity and substrate specificity of this newly identified enzyme, we have heterologously expressed MSP in a baculovirus/insect cell line system. We demonstrate that recombinant MSP exhibits a broad specificity for cleavage after arginine but not lysine residues, with kinetic characteristics intermediate between trypsin and pancreatic kallikrein. We show that the pro form of MSP does not self-activate but, rather, requires cleavage after lysine, indicating that mature active MSP is regulated by a distinct protease. MSP may be regulated in part by autolysis, since the active protein is readily inactivated through autolysis at specific internal arginine positions. Additionally, we show that MSP is abundantly expressed in inflammatory cells at sites of demyelination in the Theiler's murine encephalomyelitis virus (TMEV) model of multiple sclerosis (MS). In conjunction with data demonstrating the ability of MSP to degrade myelin-associated as well as several extracellular matrix proteins, these findings delineate MSP as a broad-specificity arginine-specific protease with the potential to play a key role in immune-mediated demyelination.

The mouse and rat kallikrein gene families are characterized by a large number of closely related members that presumably arose due to gene duplication events (*1*−*5*). The different kallikreins are characterized by a high degree of amino acid identity but different preferences for peptide substrates (*6*−*11*). Until recently, it was believed that the mouse and rat were unusual in their large number of glandular kallikrein genes and that humans had only three such genes (*12*). However, recent work indicates that humans have a large multigene family of at least 15 different kallikreins, like the mouse and rat (*13*).

Members of the kallikrein gene family exhibit differential tissue expression (*3*, *14*−*16*). Myelencephalon-specific protease (MSP)[1] is a member of the kallikrein gene family, first identified in the rat, that is primarily expressed in the brain and spinal cord and is upregulated in these tissues in response to glutamate receptor-mediated excitotoxic injury (*17*). Potential human homologues to rat MSP have also been identified and include protease M (*18*), zyme (*19*), and neurosin (*20*). Mouse homologues to MSP have been reported as brain and skin serine protease (BSSP) (*21*) and brain serine protease (BSP) (*22*). The human homologue appears to be the kallikrein referred to as human kallikrein 6 (hK6) (*23*). Studies of rat MSP and mouse protease M/neurosin have demonstrated preferential expression in oligodendrocytes (*17*, *24*, *25*). It has therefore been postulated that MSP/protease M/neurosin may play a key role in the regulation of myelin turnover and in demyelinating disease (*17*, *24*−*26*). Furthermore, it has been reported that while MSP/protease M/neurosin is detected in normal brain, it is downregulated in the brain of patients with Alzheimer's disease, suggesting that it may also play a role in the degradation of $\beta$-amyloid or turnover of amyloid precursor protein (*27*, *28*).

Although critical to understanding the role(s) of MSP in the CNS, the kinetic properties of this enzyme have not been

† This work was supported by grants from the National Multiple Sclerosis Society to M.B. (PP0757) and I.A.S. (PP0725).

* To whom correspondence should be addressed. Tel: 850-644-1863. Fax: 850-561-1406. E-mail: blaber@sb.fsu.edu.

‡ Institute of Molecular Biophysics, Florida State University.

§ Departments of Neurology and Immunology, Mayo Medical and Graduate School, Mayo Clinic Rochester.

|| Department of Chemistry and Biochemistry, Florida State University.

⊥ Department of Biological Science, Florida State University.

[1] Abbreviations: MSP, myelencephalon-specific protease; BSSP, brain and skin serine protease; BSP, brain serine protease; TMEV, Theiler's murine encephalomyelitis virus; MS, multiple sclerosis; SDS−PAGE, sodium dodecyl sulfate−polyacrylamide gel electrophoresis; EK, enterokinase; MOI, multiplicity of infection; pfu, plaque-forming unit; HPLC, high-performance liquid chromatography; MALDI, matrix-assisted laser desorption/ionization; TOF, time of flight; L-BAPNA, benzoyl-L-arginine *p*-nitroanilide; TBS, Tris-buffered saline; PBS, phosphate-buffered saline; NGS, normal goat serum; PVDF, polyvinylidene difluoride; EDTA, ethylenediaminetetraacetic acid; DMSO, dimethyl sulfoxide; AMC, aminomethylcoumarin; αMOG, myelin oligodendrocyte glycoprotein; MBP, myelin basic protein; BPT, bovine pancreatic trypsin; PPK, porcine pancreatic kallikrein.

10.1021/bi015781a CCC: $22.00 
Published on Web 12/29/2001

elucidated. We have characterized active recombinant rat MSP, produced in milligram quantities from a baculovirus/insect cell line expression system, without the need for refolding. This characterization includes the nature of the activation and autolysis of MSP, the determination of $K_m$ and $k_{cat}$ kinetic constants against a series of peptide substrates that allow direct comparison of preferences at the P1 or P2 position, and the activity of MSP against a series of myelin-related and extracellular matrix proteins. Importantly, the results show that MSP is an arginine-specific protease exhibiting broad specificity at the substrate P2 position and is subject to autocatalytic inactivation. Data are presented to show the potential activity of MSP in both tissue remodeling and demyelination, in that MSP is densely expressed by inflammatory cells at sites of demyelination in the TMEV model of MS, and MSP readily cleaves both extracellular matrix and myelin-specific proteins.

## MATERIALS AND METHODS

*Expression and Purification of Recombinant MSP*. cDNA encoding the sequence for the mature form of MSP (*17*) was inserted into the pBAC3 transfer vector (Novagen, Madison, WI) immediately 3′ to the enterokinase (EK) recognition sequence of $(Asp)_4Lys$. This resulted in a 44 amino acid synthetic prosequence (ending in the EK recognition sequence) leading into the amino-terminal Val-Val-His-Gly sequence of the mature form of MSP (*17*). Expression of MSP in the pBAC3 transfer vector utilized the BacVector transfection system (Novagen, Madison, WI). The Sf9 insect cell line, in conjunction with sf-900 II serum-free media (Life Technologies, Rockville, MD), was used for preparation of high-titer (i.e., $>10^9$ pfu/mL) viral stock. The TN5 (High5, Invitrogen Corp., Carlsbad, CA) insect cell line was used for production of expressed protein by the viral stock. Recombinant MSP protein was purified in a single step utilizing the His-tag fusion and nickel affinity resin (Ni-NTA). The eluted MSP fraction was pooled and extensively dialyzed versus 40 mM Tris-HCl, pH 7.5 (or 40 mM sodium acetate, pH 4.5), using 6−8 kDa molecular mass cutoff dialysis tubing (Spectrum Laboratories, Rancho Dominguez, CA).

*Homogeneity of Purified MSP*. Homogeneity of purified MSP was evaluated using amino-terminal sequencing, mass spectrometry, and size exclusion high-performance liquid chromatography (HPLC). For mass spectrometry the pooled fraction from the Ni-NTA column was dialyzed against 40 mM sodium acetate, pH 4.5. MALDI-TOF mass spectrometry was performed on a Bruker Biflex III mass spectrometer (Bruker Daltonics, Billerica, MA). Instrument control, data acquisition, and analysis were performed using the XACQ and XMASS software programs (Bruker Daltonics, Billerica, MA). The spectrometer was calibrated using the singly and doubly protonated molecular ion signals of equine apomyoglobin (Sigma Chemical Co., St. Louis, MO) as internal standards, and 100 laser shots were accumulated per mass spectrum. Size exclusion chromatography was performed on a Superdex 200 HR 10/30 column (Pharmacia Corp., Kalamazoo, MI) in 50 mM sodium acetate and 150 mM sodium chloride, pH 4.5. Retention times as a function of molecular mass were determined using standards of bovine serum albumin (66.4 kDa), carbonic anhydrase (29.0 kDa), and cytochrome *c* (12.4 kDa). Amino-terminal sequencing was performed on an Applied Biosystems Procise 492 protein sequencer (Applied Biosystems, Foster City, CA).

*Activation of MSP by Enterokinase*. Cleavage of the propeptide sequence from the mature MSP protein was achieved by enterokinase digestion (Roche Diagnostics Corp., Indianapolis, IN). Separation of the propeptide and enterokinase from mature MSP was performed using Sephadex G-50 gel filtration (Pharmacia Corp., Kalamazoo, MI) in 40 mM sodium acetate and 100 mM NaCl, pH 4.5. Enzymatic activity of MSP was monitored by following the hydrolysis of benzoyl-L-arginine *p*-nitroanilide substrate (L-BAPNA; Sigma Chemical Co., St. Louis, MO). The molar extinction coefficient of mature MSP was calculated as $\epsilon = 33225\ M^{-1}\ cm^{-1}$ using the method of Gill and von Hippel (*29*).

*Autolysis of MSP*. Autolysis of mature MSP and effects upon enzymatic activity were evaluated using SDS−PAGE, activity assays with L-BAPNA, and N-terminal peptide sequencing. Mature MSP in 100 mM Tris-HCl, pH 8.5, was incubated at 37 °C, and samples at time points of 0, 15, 30, 60, 90, 120, and 240 min were taken. Identical samples were evaluated using the L-BAPNA assay and 16.5% Tricine SDS−PAGE (*30*). Polypeptides resolved by the Tricine SDS−PAGE were transferred by electroblotting to polyvinylidene difluoride (PVDF) membrane (Bio-Rad Laboratories, Hercules, CA) and then subjected to amino-terminal peptide sequencing on an Applied Biosystems Procise 492 model protein sequencer (Applied Biosystems, Foster City, CA).

*Determination of Kinetic Constants*. Details of the synthesis of the peptide *p*-nitroanilide substrates will be described elsewhere. All reactions were carried out in 50 mM Tris-HCl and 0.1mM EDTA, pH 8.5 at 37 °C. The formation of the *p*-nitroanilide chromophore was monitored by absorbance at 405 nm using a Beckman Model DU640 spectrophotometer and thermostatically controlled cuvette. A molar extinction coefficient of $\epsilon = 9767\ M^{-1}\ cm^{-1}$ was used in calculating the rate of product formation (*31*). Reaction rates were determined by a linear fit to the kinetic data for the period of 100−240 s after introduction of the sample into the spectrophotometer (the initial 100 s being needed for temperature equilibration). Enzyme concentrations were chosen so as to limit substrate hydrolysis to less than 10% over the time course of the experiment. Practical substrate ranges were between 0.01 and 2 mM. Serial 1:2 dilutions (typically nine total) of substrate concentrations were chosen to cover as wide a range as possible on either side of the determined $K_m$ value for that substrate. Steady-state kinetic constants $K_m$ and $k_{cat}$ were determined from averaged duplicate data sets of initial reaction rate versus substrate concentration by nonlinear fitting to the Michaelis−Menten equation (DataFit, Oakdale Engineering, Oakdale, PA).

Hydrolysis of aminomethylcoumarin (AMC) substrates (Bachem, King of Prussia, PA) was performed in the same Tris buffer with the addition of 4% DMSO to aid solubility. Hydrolysis of the AMC substrates was monitored fluorometrically with an excitation wavelength of 380 nm and an emission wavelength of 460 nm on a Varian Cary Eclipse fluorescence spectrophotometer (Varian, Inc., Palo Alto, CA). Determination of steady-state kinetic constants followed the same procedure as with the *p*-nitroanilide substrates.

*Digestion of Myelin-Associated Proteins by MSP*. The choice of enzyme:substrate ratios used in the digestion of

protein substrates by MSP and the time course of the experiments were chosen so as to facilitate recovery of digestion fragments for amino acid sequence analysis. Rat myelin basic protein (MBP) isolated from rat spinal cord was added to MSP at a 1000:1 mass ratio in 50 mM Tris and 100 mM NaCl, pH 8.0. This mixture was incubated at 37 °C, and time points were taken at 0, 1, 2, 5, 10, 30, and 60 min. The MBP and potential degradative fragments were analyzed using Tricine SDS−PAGE (16.5%). Polypeptides resolved by the Tricine SDS−PAGE were transferred by electroblotting to PVDF membrane and subjected to amino-terminal peptide sequencing. Recombinant rat myelin oligodendrocyte glycoprotein (αMOG), consisting of the amino-terminal extracellular domain (residues 1−125), was added to MSP at a 100:1 mass ratio in 50 mM Tris and 100 mM NaCl, pH 8.0. This mixture was incubated at 37 °C, and time points taken at 0, 1, 4, and 12 h. The digested sample was resolved using Tricine SDS−PAGE (16.5%). Polypeptides resolved by the Tricine SDS−PAGE were transferred by electroblotting to PVDF membrane and subjected to amino-terminal peptide sequencing. The digested mixture from the 1 h time point was fractionated by HPLC, and the major peaks were collected and subjected to amino-terminal sequence analysis.

*Digestion of Extracellular Matrix Proteins*. Rat tail collagen type I (Sigma Chemical Co., St. Louis, MO) was reconstituted at a concentration of 5.0 mg/mL in 0.25% acetic acid. Heat-denatured soluble type I collagen (gelatin) was prepared by heating for 10 min at 95 °C in 100 mM Tris-HCl, pH 8.5. For digestion of type I collagen a final concentration of 2.9 mg/mL collagen was incubated with 0.14 mg/mL mature MSP (for a 21:1 w/w ratio of collagen:MSP). For digestion of gelatin prepared from collagen a final concentration of 2.9 mg/mL gelatin was incubated with 0.10 mg/mL mature MSP (for a 28:1 w/w ratio of gelatin:MSP). Aliquots of the digestion mix were taken at 0, 5, 30, and 60 min, resolved on 7.5% SDS−PAGE, and visualized by Coomassie blue staining.

Laminin from basement membrane of Engelbreth−Holm−Swarm mouse sarcoma (Sigma Chemical Co., St. Louis, MO) was diluted in TBS, pH 7.5, to a concentration of 1 mg/mL. Active MSP was added to a concentration of 4.2 μM (10:1 w/w ratio of laminin:MSP). The sample was incubated at 37 °C, and aliquots of the digestion mix were taken at 0, 1, and 24 h, resolved on 7.5% SDS−PAGE, and visualized by Coomassie blue staining.

Murine fibronectin (Life Technologies, Rockville, MD) was used as provided as a stock solution of 1.0 mg/mL in 2.7 mM potassium chloride, 340 mM sodium chloride, 8 mM sodium phosphate, 1.5 mM potassium phosphate, and 10% glycerol, pH 7.3. Mature MSP was added to a final concentration of 4.2 μM (10:1 w/w ratio of fibronectin:MSP). The sample was incubated at 37 °C, and aliquots were taken and analyzed in a manner identical to that of the laminin digestion.

*Immunohistochemical Localization of MSP in TMEV-Induced Demyelination.* TMEV produces chronic progressive demyelination in susceptible mice and is the most relevant available virus-induced model of immune-mediated demyelination (*32*, *33*). Six-week-old female SJL/J (H-2$^s$) mice (Jackson Laboratories, Bar Harbor, ME) were injected intracerebrally with $2 \times 10^6$ pfu of Daniel's strain of TMEV in a 10 μL volume. At 90 days postinfection, mice were perfused transcardially with 4.0% paraformaldehyde in phosphate-buffered saline (PBS, pH 7.3). Spinal cords were sectioned transversely into 1 mm blocks and embedded in paraffin.

Immunohistochemical localization of MSP in TMEV-infected spinal cord tissue was achieved using a polyclonal antibody, generated against active recombinant MSP, described herein. The antibody was generated by immunizing New Zealand White rabbits intradermally with 250 μg of active recombinant MSP in Freund's complete adjuvant, followed by 100 μg of subcutaneous boosts in Freund's incomplete adjuvant every 3 weeks over a period of 15 weeks. The IgG fraction was purified over a protein A column from the final production bleed (Covance Research Products Inc., Denver, PA). Slide-mounted 5 μm transverse paraffin sections of control or TMEV-infected spinal cords were deparaffinized, rehydrated, and processed to localize MSP and/or the macrophage marker isolectin $B_4$ (Sigma Chemical Co., St. Louis, MO), essentially as described previously (*25*, *34*). Briefly, sections were preincubated in Citra solution (BioGenex, San Ramon, CA), and nonspecific binding was blocked by incubation in 20% normal goat serum (NGS) in 0.1 M PBS for 20 min at 25 °C. The purified MSP-specific antibody was applied to tissue sections at a concentration of 5 μg/mL in 10% NGS and incubated overnight at 4 °C. After being washed in PBS, MSP-immunolabeling was visualized using standard immunoperoxidase techniques. The colocalization of MSP immunolabeling to macrophages in the same tissue section was achieved by application of fluorescein- (FITC-) conjugated isolectin $B_4$ (diluted 1:50 in 10% NGS). Tissue sections were finally washed in PBS, rinsed in doubly distilled $H_2O$, and cover slipped with 90% glycerol (pH 8.0). No immunostaining was observed in the absence of primary antibody, and the newly generated rabbit polyclonal antibodies used in this study yielded staining patterns identical to those obtained using monoclonal antibodies generated against MSP-specific peptides (*25*, *34*). Sections were viewed on an Olympus AX70 microscope, using transmitted light to view MSP-specific peroxidase labeling, and under fluorescence (excitation 460−490 nm, emission 515−550 nm) to view FITC-conjugated isolectin $B_4$, in the same tissue section. All images were collected digitally with a SPOT digital camera (Diagnostic Instruments, Sterling Heights, MI).

*Western Blotting of MSP in Tissue Homogenates*. Tissue homogenate from rat spinal cord, brain, and kidney was thawed on ice and centrifuged at 20000 rpm for 30 min at 4 °C. Twenty microliters of cleared homogenates and 10 ng of active rMSP control were loaded onto a 15% SDS−PAGE gel. Transblotting onto PVDR membrane was carried out in 10 mM 3-(cyclohexylamino)-1-propanesulfonic acid, 0.005% (w/v) SDS, and 10% methanol, pH 11.05, at 80 V for 3 h. Hybridization and detection were carried out according to the manufacturer's protocol with 3% gelatin in TBS (pH 7.6) and 0.1% Tween 20 as a blocking agent (ECL Western blotting analysis system, Amersham Pharmacia Biotech, Piscataway, NJ). The primary antibody was rabbit polyclonal raised against the active form of rMSP at 1:2000 dilution with TBS (pH 7.6) and 0.1% Tween 20. The secondary antibody was horseradish peroxidase-conjugated donkey anti-rabbit at a dilution of 1:10000 with TBS (pH 7.6) and 0.1%

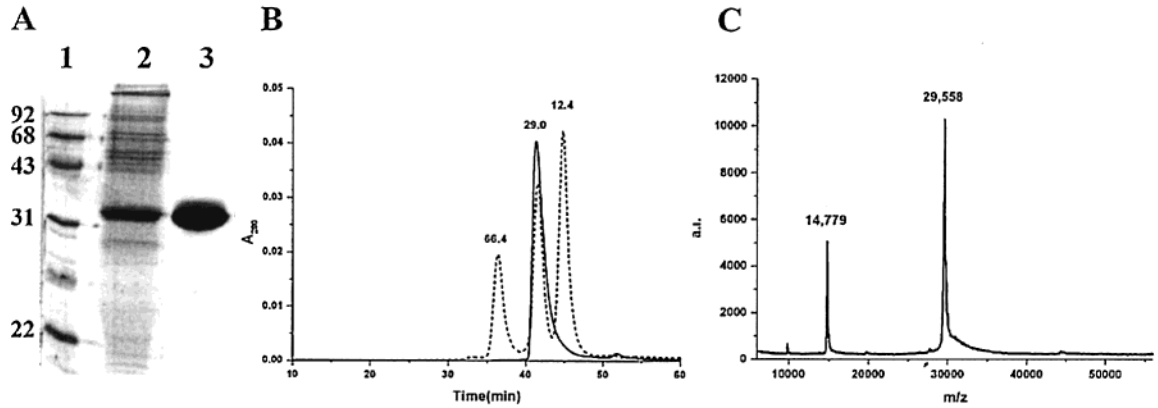


FIGURE 1: Purified recombinant MSP is a homogeneous protein with no prosthetic groups. Panel A: Expressed and purified recombinant pro-MSP. Lanes: 1, molecular mass markers; 2, insect cell culture media at 48 h postinfection (the major band is MSP); 3, purified recombinant pro-MSP. Panel B: HPLC analysis of recombinant pro-MSP (solid line) overlaid onto the HPLC trace (dotted line) for molecular mass markers bovine serum albumin (66.4 kDa), carbonic anhydrase (29.0 kDa), and cytochrome *c* (12.4 kDa). Panel C: Mass spectrogram of purified recombinant pro-MSP, with an indicated molecular mass of 29.558 kDa. Also shown is a peak at 14.779 kDa that represents intact MSP at one-half the *m*/*z* ratio.

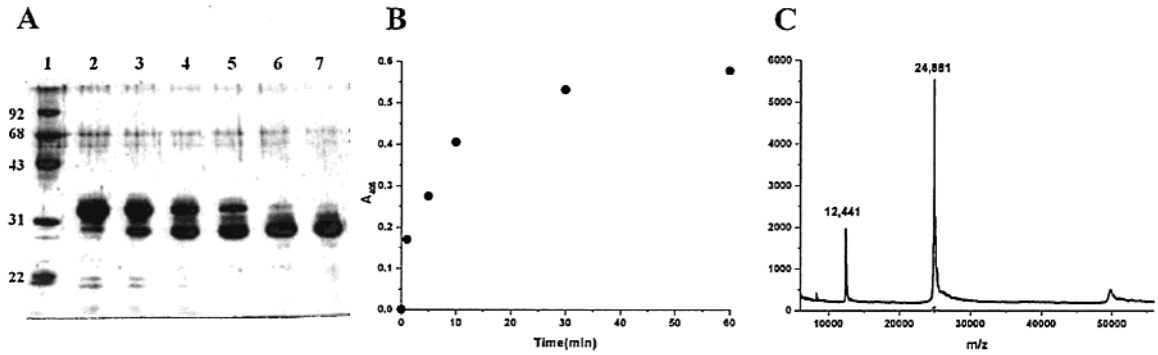


FIGURE 2: Activation at the synthetic enterokinase cleavage site produces mature, enzymatically active MSP. Panel A: 15% SDS−PAGE analysis of a time course of activation of pro-MSP by enterokinase. Lanes: 1, molecular mass markers; 2, $T_0$ time point; 3, 1 min; 4, 5 min; 5, 10 min; 6, 30 min; 7, 60 min. Panel B: Enzymatic activity against L-BAPNA for samples of the time course of activation of pro-MSP by enterokinase in panel A. Panel C: Mass spectrogram of purified mature MSP with an indicated molecular mass of 24.881 kDa. Also shown is a peak at 12.441 kDa that represents intact mature MSP at one-half the *m*/*z* ratio (a minor peak at approximately 49.8 kDa represents intact mature MSP at twice the *m*/*z* ratio).

Tween 20. Autoradiography was performed using Kodak X-Omar scientific imaging film.

## RESULTS

*Expression and Purification of Recombinant MSP.* Optimal expression of recombinant MSP was achieved using a multiplicity of infection of 1.0 and harvesting the culture supernatant at 48 h postinfection (Figure 1). The MSP eluting from the Ni-NTA resin was judged to be better than 98% pure by Coomassie blue stained SDS−PAGE, resulting in essentially a single-step purification (Figure 1). The typical yield of purified MSP zymogen was between 10 and 25 mg/L of TN5 culture media.

*Homogeneity of Purified MSP.* Amino-terminal sequence analysis of the purified MSP zymogen revealed that the first five amino acids were alanine, methionine, valine, histidine, and histidine. This sequence matched the first five amino acids of the vector-derived 44 amino acid propeptide sequence and indicated that the expressed MSP was correctly cleaved after the anticipated signal peptide recognition sequence (and secreted into the media). MALDI-TOF mass spectroscopy analysis resulted in a single peak with a mass of 29558 Da (Figure 1). This agrees very well with the calculated molecular mass for the secreted pro form (with synthetic propeptide sequence) of 29552 Da. The results of size exclusion chromatography for the purified pro-MSP show a single peak eluting at 41.1 min, or a slightly larger apparent mass compared to the carbonic anhydrase standard (retention time of 41.4 min and mass 29025 Da). The mass spectroscopy and HPLC results indicate that there is no posttranslational modification such as glycosylation or proteolysis of the purified pro-MSP. The results also indicate that the native state of the MSP is entirely monomeric and homogeneous, with no significant aggregated states or disulfide-linked multimers.

*Activation of MSP by Enterokinase and Autolysis of MSP.* Addition of enterokinase to the purified synthetic pro form of MSP resulted in the hydrolysis of the polypeptide chain with production of an ∼24 kDa mass peptide as determined by SDS−PAGE (Figure 2). However, cleavage of the propeptide by added enterokinase at pH 7.0−8.0 was quickly followed by an additional internal cleavage in the mature MSP. This secondary cleavage event was prevented by lowering the pH to 4.5 during enterokinase treatment (30−60 min at 37 °C). After removal of residual enterokinase and the ∼6 kDa propeptide fragment by gel filtration, the mature MSP remained a single-chain form at pH 4.5. Mass spectroscopy analysis of the G-50 purified active form of

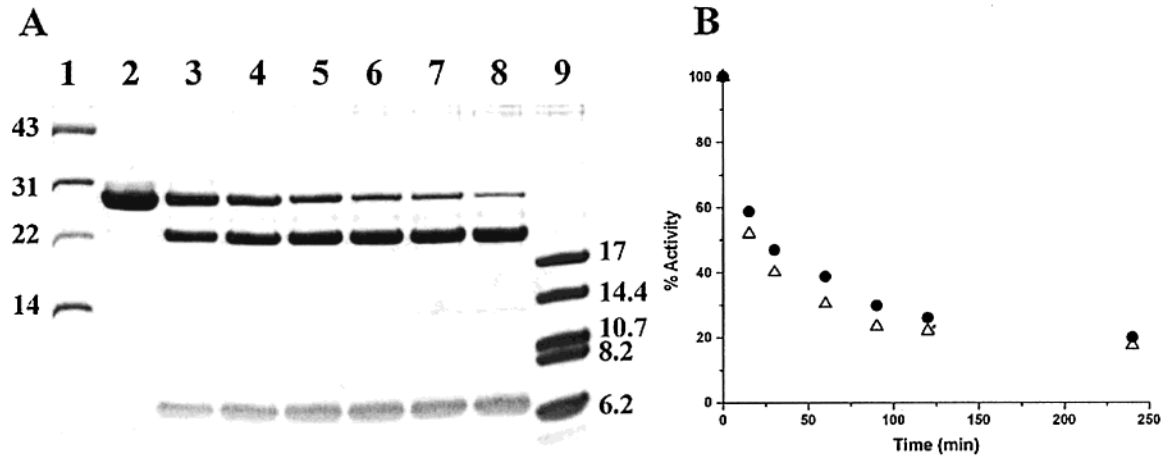


FIGURE 3: Mature MSP can autolyze, resulting in a loss of enzymatic activity. Panel A: 16.5% Tricine SDS−PAGE (run under reducing conditions) showing a time course profile of autolysis of activated MSP (20.8 $\mu$M) in 0.10 M Tris, pH 8.5. Lanes: 1 and 9, molecular mass markers; 2, purified active MSP at 0 time point; 3, 15 min; 4, 30 min; 5, 60 min; 6, 90 min; 7, 120 min; 8, 240 min incubation time point. Panel B: Normalized integrated values for single-chain MSP from panel A (closed circles) and normalized enzymatic activity against L-BAPNA for samples in panel A (open triangles).

Table 1: Kinetic Constants for Hydrolysis of L-BAPNA by Mature MSP (50 mM Tris, 0.1 mM EDTA, pH 8.5, 37 °C)[a]

| enzyme | $K_m$ ($\mu$M) | $k_{cat}$ ($s^{-1}$) | $k_{cat}/K_m$ ($\times 10^3$ $M^{-1}$ $s^{-1}$) |
|---|---|---|---|
| MSP | 304 ± 17 | 0.0658 ± 0.0013 | 0.216 |
| mGK-9 | 241 | 1.78 | 7.4 |
| mGK-3 | 35.7 | 1.80 | 50.4 |
| BPT | 368 | 2.69 | 7.3 |
| PPK | 383 | 0.154 | 0.402 |

[a] Included are kinetic constants reported under identical conditions for the mouse glandular kallikreins mGK-3 ($\gamma$-subunit of nerve growth factor), mGK-9 (epidermal growth factor binding protein), bovine trypsin (BPT), and porcine kallikrein (PPK) (*6*).

MSP showed a single peak with a mass of 24881 Da, in excellent agreement with the calculated mass of 24897 (Figure 2). Amino-terminal analysis yielded the correct mature sequence of Val-Val-His-Gly (*17*).

Incubation of purified mature MSP at pH 7.0, or higher, resulted in the internal cleavage observed during enterokinase activation and concomitant reduction in yield of enzymatic activity. Amino-terminal sequencing of the SDS−PAGE-resolved fragments identified two adjacent peptide sequences, in essentially equimolar concentrations, corresponding to a cleavage between residues arginine 74 and glutamine 75 and between residues arginine 81 and glutamine 82 (numbering scheme of chymotrypsin). A time course of these autolysis events demonstrated that enzymatic activity against L-BAPNA decreased simultaneously with generation of these internal cleavages (Figure 3). SDS−PAGE in the presence and absence of $\beta$-mercaptoethanol indicated that disulfide bonds were formed between the fragmented regions of the protein, as is predicted from the characteristic disulfide bond pattern in serine-type proteases (data not shown).

*Determination of Steady-State Kinetic Constants.* Kinetic constants for the hydrolysis of L-BAPNA by the processed mature form of MSP are listed in Table 1. The active MSP exhibited characteristic Michaelis−Menten kinetics with all substrates. No hydrolysis of L-BAPNA was observed with the pro form. Kinetic constants for the hydrolysis of the tripeptide substrates N-Ac-Glu-Leu-Arg-pNa (AcELRpNa) and N-Ac-Ala-Thr-Arg-pNa (AcATRpNa) are listed in Table 2, and hydrolysis of the AMC tripeptide substrates are listed in Table 3.

Table 2: Kinetic Constants for Hydrolysis of Tripeptide Nitroanilide Substrates N-Ac-Glu-Leu-Arg-pNa (AcELRpNa) and N-Ac-Ala-Thr-Arg-pNa (AcATRpNa) by Mature MSP (50 mM Tris, 0.1 mM EDTA, pH 8.5, 37 °C)[a]

| enzyme | substrate | $K_m$ ($\mu$M) | $k_{cat}$ ($s^{-1}$) | $k_{cat}/K_m$ ($\times 10^3$ $M^{-1}$ $s^{-1}$) |
|---|---|---|---|---|
| MSP | AcELRpNa | 296 ± 6 | 4.05 ± 0.04 | 13.7 |
| | AcATRpNa | 176 ± 14 | 4.13 ± 0.13 | 23.5 |
| mGK-9 | AcELRpNa | 74.1 | 51.5 | 695 |
| | AcATRpNa | 506 | 17.8 | 35.2 |
| mGK-3 | AcELRpNa | 23.8 | 14.3 | 601 |
| | AcATRpNa | 93.5 | 29.0 | 310 |
| BPT | AcELRpNa | 187 | 42.9 | 229 |
| | AcATRpNa | 52.9 | 21.1 | 399 |
| PPK | AcELRpNa | 849 | 9.2 | 10.8 |
| | AcATRpNa | 571 | 0.72 | 1.26 |

[a] Also included are kinetic constants reported under identical conditions for the mouse glandular kallikreins mGK-3 ($\gamma$-subunit of nerve growth factor), mGK-9 (epidermal growth factor binding protein), bovine trypsin (BPT), and porcine kallikrein (PPK) (*6*).

Table 3: Kinetic Constants for Hydrolysis of Tos-Gly-Pro-Arg and Tos-Gly-Pro-Lys AMC Substrates by Mature MSP (50 mM Tris, 0.1 mM EDTA, 4% DMSO, pH 8.5, 37 °C)[a]

| enzyme | substrate | $K_m$ ($\mu$M) | $k_{cat}$ ($s^{-1}$) | $k_{cat}/K_m$ ($\times 10^3$ $M^{-1}$ $s^{-1}$) |
|---|---|---|---|---|
| MSP | Tos-GPR-AMC | 408 ± 19 | 3.53 ± 0.08 | 35.3 |
| | Tos-GPK-AMC | 269 ± 10 | 0.13 ± 0.01 | 0.48 |
| BPT | Tos-GPR-AMC | 3.5 ± 0.5 | 29 ± 1 | 8286 |
| | Tos-GPK-AMC | 12.3 ± 1.2 | 16.9 ± 0.8 | 1373 |

[a] Also included are kinetic constants reported under similar conditions for bovine trypsin (*35*).

*Digestion of Myelin-Associated Proteins by MSP.* Rat myelin basic protein (MBP) was extensively degraded by MSP such that no fragments resolvable on 20% SDS−PAGE remained after overnight digestion. During the initial incubation period a characteristic pattern of four lower molecular mass fragments emerged during the digestion (fragments A−D, Figure 4). Sequence analysis indicated that fragments A and D share the same amino terminal sequence, while fragments B and C are uniquely different (Table 4). Rat

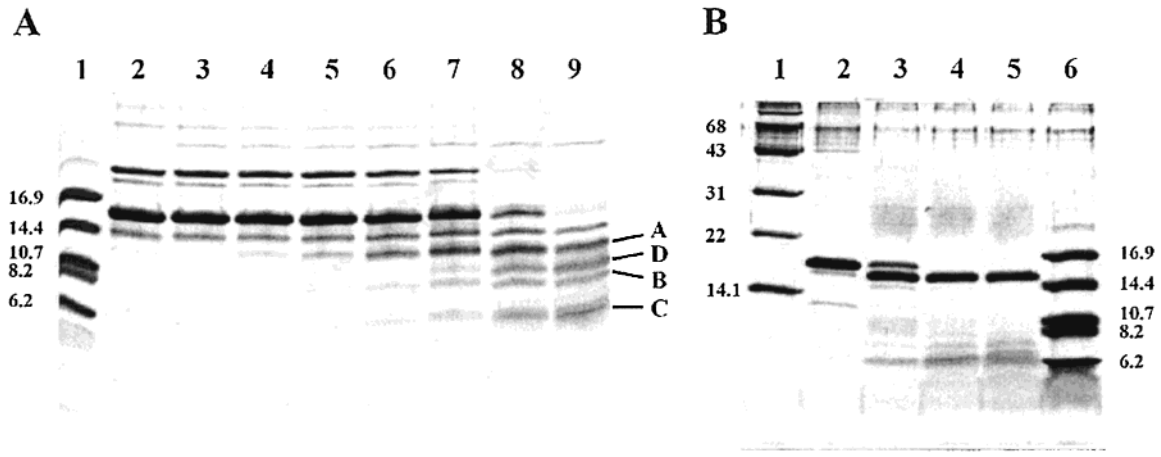


FIGURE 4: Degradation of myelin-related proteins by MSP. Panel A: 16.5% Tricine SDS−PAGE showing the time course digest of rat MBP by MSP. Lanes: 1, low molecular mass protein markers; 2, no MSP; 3, 0 min; 4, 1 min; 5, 2 min; 6, 5 min; 7, 10 min; 8, 30 min; 9, 60 min incubation with MSP. Panel B: 16.5% Tricine SDS−PAGE showing the time course digest of the rat myelin oligodendrocyte glycoprotein (αMOG) external fragment (residues 1−125) by MSP (1:100 w/w ratio). The digest was performed at 37 °C in 100 mM Tris-buffered saline, pH 8.0. Lanes: 1, molecular mass markers; 2, 0 min; 3, 1 h; 4, 4 h; 5, 12 h; 6, molecular mass markers.

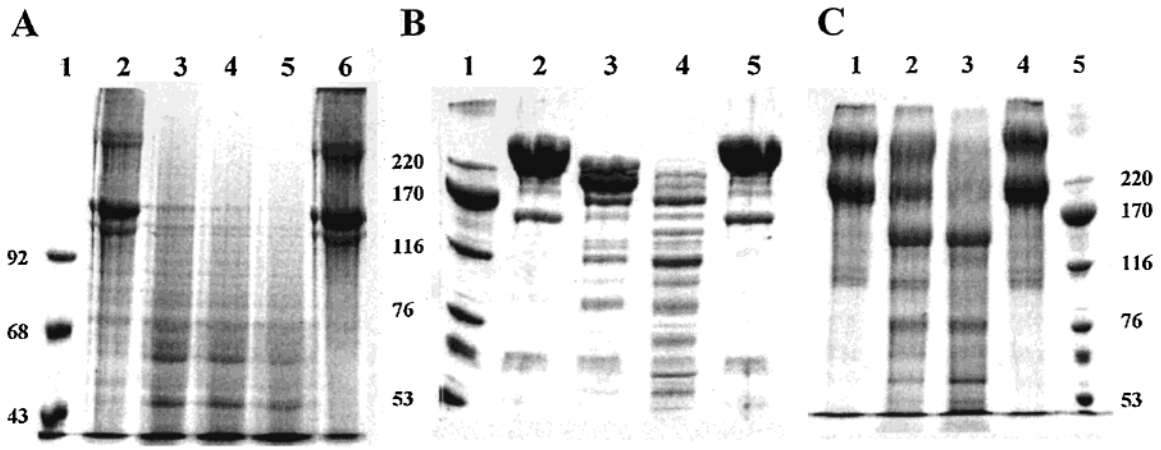


FIGURE 5: Degradation of extracellular matrix proteins by MSP. Panel A: 7.5% SDS−PAGE (reducing) showing heat-denatured collagen type I by MSP. Lanes: 1, molecular mass standards (kDa); 2, gelatin + MSP, 0 min; 3, gelatin + MSP, 5 min; 4, gelatin + MSP, 30 min; 5, gelatin + MSP, 60 min; 6, gelatin alone, 60 min incubation at 37 °C. Panel B: 7.5% SDS−PAGE showing digestion of 60 $\mu$g of fibronectin by 6 $\mu$g of MSP at 37 °C in 2.7 mM KCl, 340 mM NaCl, 8 mM sodium phosphate, 1.5 mM potassium phosphate, and 10% glycerol, pH 7.3. Lanes: 1, high molecular mass markers; 2, fibronectin plus MPS, 0 h; 3, fibronectin plus MSP, 1 h; 4, fibronectin plus MSP, 24 h; 5, fibronectin control, 24 h. Panel C: 7.5% SDS−PAGE (reducing) showing the laminin digest by MSP. Lanes: 1, laminin + MSP, 0 h; 2, laminin + MSP, 1 h; 3, laminin + MSP, O/N; 4, laminin control, O/N; 5, high molecular weight protein marker.

αMOG exhibited a rapid cleavage event upon incubation with MSP that reduced the molecular mass from 15.5 to 14.7 kDa (Figure 4). However, amino-terminal sequencing shows this cleavage site to be within an amino-terminal leader sequence derived from the cloning vector polylinker. Internal sites of the αMOG protein are much more resistant to cleavage. However, slow hydrolysis at several internal sites is apparent (Figure 4). Amino acid sequence analysis indicates the presence of at least seven internal sites of cleavage by MSP. These sites all occur after arginine residues and contain phenylalanine, isoleucine, tyrosine, serine, or valine at the P2 position.

*Digestion of Extracellular Matrix Proteins.* Intact rat collagen type I exhibited no apparent digestion by MSP. Heat-denatured collagen type I (gelatin), however, was rapidly degraded over the course of several minutes (Figure 5). Mouse laminin was also rapidly degraded by MSP, yielding a protease-resistant polypeptide of ∼140 kDa and numerous small polypeptide fragments (Figure 5). Rat plasma fibronectin was rapidly degraded to a polypeptide with an apparent molecular mass of ∼200 kDa. This polypeptide was subsequently degraded to numerous smaller fragments after overnight digestion (Figure 5).

Table 4: Amino-Terminal Sequence Analysis of Early Digest Fragments of MBP by Mature MSP[a]

| fragment | P2 residue | P1 residue | sequence |
|---|---|---|---|
| A | P | R | HRDTGI |
| B | T | R | TTHYGS |
| C | H | R | DTGILD |
| D | P | R | HRDTGI |

[a] Fragment identification follows that of Figure 4.

*MSP Immunoreactivity in TMEV-Induced Demyelination.* We have previously shown that MSP is densely expressed by oligodendroglia of the adult rodent and human spinal cord white matter (*17*, *25*, *34*). This is confirmed in the present

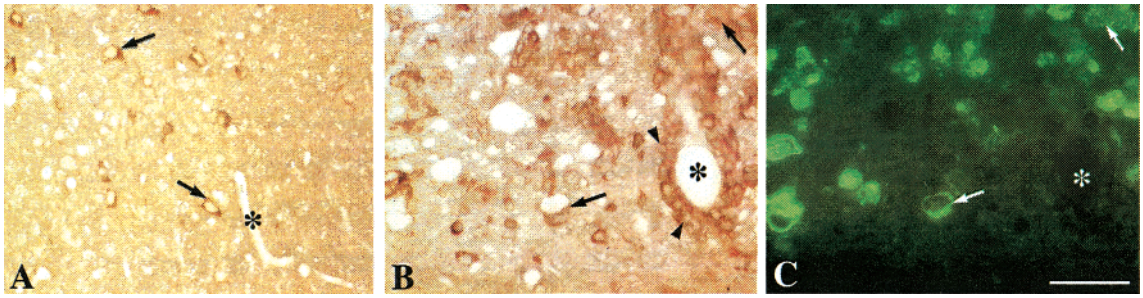


FIGURE 6: The localization of MSP in normal and diseased spinal cord suggests a role in demyelination. Panel A: In normal adult mouse spinal cord white matter MSP immunoreactivity is associated with oligodendrocytes, a subset of which are indicated at the arrows. Panel B: The typical pattern of MSP immunoreactive cells (arrows and arrowheads) present at sites of focal inflammation and demyelination 90 days following TMEV infection. Panel C: The same section as in panel B stained by immunofluorescence for the macrophage marker isolectin $B_4$. Arrows in panels B and C point to some of the macrophages identified in panel C, which are also MSP immunoreactive. MSP immunoreactivity among inflammatory cells was not limited to macrophages, however, since many MSP immunoreactive inflammatory cells contained within perivascular cuffs (arrowheads, panel B) were not isolectin $B_4$ positive. Asterisks in each panel indicate a blood vessel, which is associated with inflammatory cells following TMEV infection but not in normal cord white matter. Scale bar = 50 $\mu$m.

study (Figure 6, panel A) using newly generated polyclonal antibodies raised against the active recombinant MSP protein. Examination of the spinal cord white matter of mice 90 days following infection with TMEV revealed dense immunostaining for MSP associated with inflammatory cells, both within perivascular cuffs and within the substance of the cord white matter at sites of demyelination (Figure 6, panel B). Immunostaining of the same tissue section for the macrophage marker, isolectin $B_4$, indicated that many, but not all, MSP immunoreactive inflammatory cells were also isolectin B4 positive (Figure 6, panel C).

## DISCUSSION

The original hypothesis of MSP activity, as deduced from amino acid sequence information, was that MSP would be a broad-specificity trypsin-like digestive protease (*17*). Given that MSP is abundantly expressed in the brain and spinal cord and is upregulated in response to glutamate receptor-mediated excitotoxic injury, the potentially broad substrate specificity of this enzyme is of considerable significance with regard to the maintenance of normal brain function. While MSP has not previously been characterized, some general enzymatic properties of a related mouse protease (mouse brain serine protease, 88% identity with MSP) have been reported (*22*). Although this protease (isolated from an *Escherichia coli* expression host) required refolding to demonstrate activity, and $K_m$ and $k_{cat}$ kinetic constants were not determined, analysis of various peptide substrates suggested a general preference for cleavage after arginine residues. Thus, one of the goals of the present study was to quantitate the preference of lysine or arginine in the P1 position, as well as the influence of chemically disparate residues in the P2 position.

The preference for arginine versus lysine at the substrate P1 positions was quantitated by determination of kinetic constants $K_m$ and $k_{cat}$ and comparing the catalytic efficiency ($k_{cat}/K_m$) toward a lysine aminomethylcoumarin substrate compared to the arginine homologue (Table 3). MSP is shown to have a 74-fold greater catalytic efficiency for cleavage after arginine compared to lysine residues in a peptide substrate. Thus, MSP does not have as broad a specificity at the P1 position in comparison to trypsin and is more similar to proteases such as porcine kallikrein or thrombin in being selective for arginine over lysine at this position (*36*−*38*). This P1 site specificity distinction in comparison with trypsin also extends to overall catalytic efficiency. MSP is much more similar in this regard to porcine kallikrein than to trypsin, as determined by catalytic efficiency toward L-BAPNA or tripeptide substrates (Tables 1 and 2).

Determination of kinetic constants for peptide substrates with identical P1 residues, and different P2 residue positions, as well as sequence analysis of the cleavage sites in protein substrates, allowed us to evaluate the P2 site specificity of MSP. These results showed that there is little apparent preference at the substrate P2 position. Residues in the P2 position at the sites of autolysis included leucine and glutamine. Residues in the P2 position at the cleavage sites of MBP included proline, threonine, and histidine (Table 4), and the limited digest of αMOG occurs at arginine residues with a variety of residues (mostly hydrophobic) at the P2 position. Furthermore, MSP exhibits a similar catalytic efficiency toward two tripeptide substrates tested with chemically different types of residues at the P2 position (leucine versus threonine). Together, these data suggest little distinction between hydrophobic, polar, basic, or acidic residues at the P2 position. Selectivity for arginine in the P1 position and minimal discrimination at the P2 position suggest that MSP can be characterized as a serine protease, selectively expressed in the CNS, that selectively targets arginine-containing peptides for degradation. MBP is a myelin-associated protein that is rich in arginine residues with a variety of different amino acids on either side of these arginines. Such a protein would therefore be predicted to be efficiently degraded by MSP. The incubation of MSP with MBP demonstrates that MSP rapidly degrades MBP due to hydrolysis at essentially all of the internal arginine positions (Figure 4).

Being an arginine-specific degradative type protease, with a demonstrated ability to hydrolyze a variety of extracellular matrix and central nervous system-specific proteins, suggests that the unregulated activity of MSP in the CNS could be highly deleterious to normal brain function. Here we have studied changes in MSP immunoreactivity which ensue following infection with TMEV, known to produce CNS demyelinating disease that closely resembles plaques present in human MS. We have demonstrated that MSP is localized to inflammatory cells at sites of demyelination, including

macrophages, known to actively degrade myelin debris. Additionally, in conjunction with data showing that MSP cleaves all of the main components of the blood brain barrier, i.e., laminin, fibronectin, and type IV collagen, we hypothesize that an additional function of MSP production by inflammatory cells may be to facilitate the extravasation of inflammatory cells into the CNS. While several mechanisms may be required to initiate clinical disease in MS, the data presented suggest that MSP may be one of the effector molecules mediating both inflammation and myelin breakdown. Understanding the regulatory cascade governing the enzymatic activity of MSP, therefore, becomes important not only to our understanding of its function in the normal CNS but also to the contribution it may make to immune-mediated demyelination.

Natural MSP is expressed as a pro form with an amino-terminal activation peptide sequence of Ser-Glu-Asp-Gln-Asp-Lys (*17*). Activation requires proteolytic cleavage after the lysine residue in this propeptide. In addition to construction of the enterokinase recognition sequence [$(Asp)_4Lys$] as the MSP propeptide, expression of the natural activation hexapeptide was also evaluated. While the natural prosequence construct yielded equivalent amounts of expressed protein, MSP was not able to self-activate. Addition of small amounts of mature active MSP resulted in cleavage at the internal autolysis site(s) rather than cleavage of the prosequence. In total, these results indicate that the activation of MSP is tightly regulated in the CNS, occurring through the action of an enterokinase-like lysine-specific regulatory protease in the brain and spinal cord.

One of the properties of active MSP demonstrated in this report is the ability to efficiently autolyze at two adjacent internal sites (after residues Arg74 and Arg81). A comparison of the progress of cleavage and the loss of enzymatic activity toward L-BAPNA suggests that these internal cleavages result in a form of MSP with no apparent residual enzymatic activity (Figure 3). This is similar to the regulatory feature of rat trypsin, which can autocatalytically inactivate by internal cleavages between residues Lys61-Ser62 and Arg117-Val118 (*39*−*41*). This is also in contrast to the various autolytic sites in the mouse glandular kallikreins, which occur without inactivation of the enzymes (*42*, *43*). The autolysis sites within trypsin function as a regulatory mechanism, and mutations that abolish this autolysis may be responsible for one type of pancreatitis (*41*, *44*). Thus, we postulate that the autolysis observed in MSP represents a similar regulatory mechanism, which likely contributes to the tight regulation of its activity in the brain.

In addition to autolysis, MSP is also likely to be regulated by formation of an inhibitor complex. Western blots of brain, spinal cord, and kidney tissues using a rabbit polyclonal antisera raised against recombinant MSP indicate the presence of high molecular mass MSP cross-reacting material. These findings suggest the presence of SDS-resistant MSP/inhibitor complexes, with derived masses of approximately 42 and 91 kDa (Figure 7). The larger 91 kDa complex is found primarily in the kidney, whereas the 42 kDa complex is found predominantly in the brain and spinal cord, suggesting the possibility of unique MSP inhibitors in neural compared with nonneural tissues. Taking into account an apparent PAGE mass of 25 kDa for mature MSP on SDS−PAGE, the mass of the associated binding protein(s) would be approximately 17 kDa for brain and 66 kDa for kidney. An important goal of future studies will be to identify and characterize these complexes.

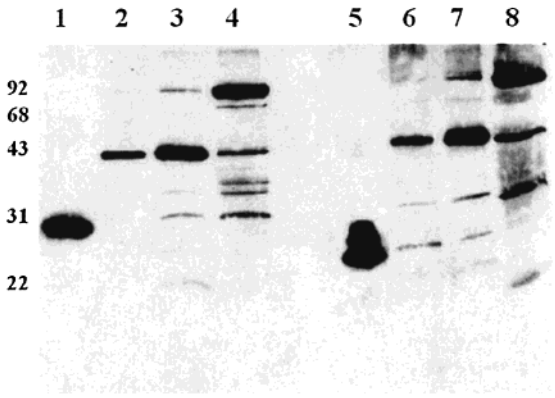


FIGURE 7: Western blot from 15% PAGE using rabbit polyclonal antibodies against recombinant MSP suggests complex formation with specific inhibitors. Lanes: 1, 10 ng of recombinant MSP; 2, 2.2 $\mu$g/$\mu$L rat spinal cord homogenate; 3, 6.4 $\mu$g/$\mu$L rat brain homogenate; 4, 9.6 $\mu$g/$\mu$L rat kidney homogenate; 5−8, identical to lanes 1−4 but with the omission of $\beta$-mercaptoethanol.

Although both rat MSP and its human homologue, hK6, are preferentially expressed in the brain, significant levels of the enzyme are also present in other organs. Levels of hK6 have been shown to be upregulated both in primary ovarian tumor tissue (*18*) and in the sera of ovarian cancer patients (*23*). Notably, tumor growth and invasion are associated with the degradation of extracellular matrix barriers, including laminin and fibronectin. Taken with the demonstration in the present study that MSP rapidly and specifically degrades both laminin and fibronectin, these data support the view that increased levels of MSP may participate in tumor pathogenesis or progression.

The rapid degradation of MBP by MSP, the preferential expression of MSP in oligodendroglia within the white matter of the normal adult human brain (*26*), and the high levels of MSP associated with inflammatory cells at sites of immune-mediated demyelination point to a role for MSP in myelin homeostasis and also potential demyelination. As an additional consideration, peptide fragments of MBP can induce a T-cell-mediated inflammatory response, referred to as experimental autoimmune encephalomyelitits (EAE), producing an MS-like demyelinating pathology (*45*). The efficient degradation of MBP by MSP and the association of MSP with inflammatory cells at sites of demyelination suggest that MSP-driven MBP degradation could generate encephalitogenic epitopes, which may contribute to the pathogenesis of MS. αMOG, a transmembrane glycoprotein, with a single Ig-like extracellular amino-terminal domain, is localized on the surface of myelin sheaths (*46*). This compact, disulfide-stabilized structure appears to be more resistant to digestion by MSP than MBP. Nevertheless, MSP was able to slowly degrade αMOG. Studies have shown that the amino-terminal extracellular domain can stimulate autoimmune-mediated demyelination (*47*−*49*). Thus, the activity of MSP against both MBP and αMOG, together with its demonstrated abundant expression in the adult CNS, supports the hypothesis that MSP plays a role in myelin turnover (*17*, *25*, *26*), both in the normal brain and in demyelinating disease. These data further underscore the importance of

understanding the regulatory mechanisms of this enzyme, which could potentially be harnessed to affect brain pathology.

## ACKNOWLEDGMENT

The authors thank Dr. Christopher Linington for generously providing the αMOG expression plasmid and Dr. Hyun I. Park for helpful discussions.

## REFERENCES

1. Evans, B. A., Drinkwater, C. C., and Richards, R. I. (1987) *J. Biol. Chem. 262*, 8027−8034.
2. Mason, A. J., Evans, B. A., Cox, D. R., Shine, J., and Richards, R. I. (1983) *Nature 303*, 300−307.
3. Wines, D. R., Brady, J. M., Pritchett, D. B., Roberts, J. L., and MacDonald, R. J. (1989) *J. Biol. Chem. 264*, 7653−7662.
4. Wines, D. R., Brady, J. M., Southard, E. M., and MacDonald, R. J. (1991) *J. Mol. Evol. 32*, 476−492.
5. Gerald, W. L., Chao, J., and Chao, L. (1986) *Biochim. Biophys. Acta 866*, 1−14.
6. Blaber, M., Isackson, P. J., James C. Marsters, J., Burnier, J. P., and Bradshaw, R. A. (1989) *Biochemistry 28*, 7813−7819.
7. Frey, P., Forand, R., Maciag, T., and Shooter, E. M. (1979) *Proc. Natl. Acad. Sci. U.S.A. 76*, 6294−6298.
8. Hosoi, K., Tsunasawa, S., Kuihara, K., Aoyama, H., Ueha, T., Murai, T., and Sakyama, F. (1994) *J. Biochem. 115*, 137−143.
9. Jongstra-Bilen, J., Coblenz, L., and Shooter, E. M. (1989) *Brain Res. Mol. Brain Res. 5*, 159−169.
10. Kim, W.-S., Nakayama, K., Nakagawa, T., Kawamura, Y., Haraguchi, K., and Murakami, K. (1991) *J. Biol. Chem. 266*, 19283−19287.
11. Wilson, W. H., and Shooter, E. M. (1979) *J. Biol. Chem. 254*, 6002−6009.
12. Riegman, P. H., Vlietstra, R. J., Suurmeijer, L., Cleutjens, C. B., and Trapman, J. (1992) *Genomics 14*, 6−11.
13. Yousef, G. M., and Diamandis, E. P. (2001) *Endocr. Rev. 22*, 184−204.
14. MacDonald, R. J., Southard-Smith, E. M., and Kroon, E. (1996) *J. Biol. Chem. 271*, 13684−13690.
15. van Leeuwen, B. H., Evans, B. A., Tregear, G. W., and Richards, R. I. (1986) *J. Biol. Chem. 261*, 5529−5535.
16. Penschow, J. D., Drinkwater, C. C., Haralambidis, J., and Coghlan, J. P. (1991) *Mol. Cell. Endocrinol. 81*, 135−146.
17. Scarisbrick, I. A., Towner, M. D., and Isackson, P. J. (1997) *J. Neurosci. 17*, 8156−8168.
18. Anisowicz, A., Sotiropoulou, G., Stenman, G., Mok, S. C., and Sager, R. (1996) *Mol. Med. 2*, 624−636.
19. Little, S. P., Dixon, E. P., Norris, F., Buckley, W., Becker, G. W., Johnson, M., Dobbins, J. R., Wyrick, T., Miller, J. R., MacKellar, W., Hepburn, D., Corvalan, J., McClure, D., Liu, X., Stephenson, D., Clements, J., and Johnstone, M. (1997) *J. Biol. Chem. 272*, 25135−25142.
20. Yamashiro, K., Tsuruoka, N., Kodama, S., Tsujimoto, M., Yamamura, Y., Tanaka, T., Nakazato, H., and Yamaguchi, N. (1997) *Biochim. Biophys. Acta 1350*, 11−14.
21. Meier, N., Dear, T. N., and Boehm, T. (1999) *Biochem. Biophys. Res. Commun. 258*, 374−378.
22. Matsui, H., Kimura, A., Yamashiki, N., Moriyama, A., Kaya, M., Yoshida, I., Takagi, N., and Takahashi, T. (2000) *J. Biol. Chem. 275*, 11050−11057.
23. Diamandis, E. P., Yousef, G. M., Soosaipillai, A. R., and Bunting, P. (2000) *Clin. Biochem. 33*, 579−583.
24. Yamanaka, H., He, X., Matsumoto, K., Shiosaka, S., and Yoshida, S. (1999) *Mol. Brain Res. 71*, 217−224.
25. Scarisbrick, I. A., Asakura, K., Blaber, S., Blaber, M., Isackson, P. J., Bieto, T., Rodriguez, M., and Windebank, A. J. (2000) *Glia 30*, 219−230.
26. Scarisbrick, I., Isackson, P. J., Ciric, B., Windebank, A. J., and Rodriguez, M. (2001) *J. Comp. Neurol. 431*, 347−361.
27. Ogawa, K., Yamada, T., Tsujioka, Y., Taguchi, J., Takahashi, M., Tsuboi, Y., Fujino, Y., Nakajima, M., Yamagoto, T., Akatsu, H., Mitsui, S., and Yamaguchi, N. (2000) *Psychiatry Clin. Neurosci. 54*, 419−426.
28. Diamandis, E. P., Yousef, G. M., Petraki, C., and Soosaipillai, A. R. (2000) *Clin. Biochem. 33*, 663−667.
29. Gill, S. C., and von Hippel, P. H. (1989) *Anal. Biochem. 182*, 319−326.
30. Dayhuff, T. J., Gesteland, R. F., and Atkins, J. F. (1992) *BioTechniques 13*, 500−503.
31. Lottenberg, R., and Jackson, C. M. (1983) *Biochim. Biophys. Acta 742*, 558−564.
32. Lindsley, M. D., and Rodriquez, M. (1989) *J. Immunol. 142*, 2677−2682.
33. Miller, S. D., and Gerety, S. J. (1990) *Semin. Virol. 1*, 263−272.
34. Scarisbrick, I. A., Blaber, S. I., Lucchinetti, C. F., Genain, C. P., Blaber, M., and Rodriguez, M. (2001) *Brain* (in press).
35. Hedstrom, L., Lin, T.-Y., and Fast, W. (1996) *Biochemistry 35*, 4515−4523.
36. Fiedler, F., Fink, E., Tschesche, H., and Fritz, H. (1981) *Methods Enzymol. 80*, 493−532.
37. Harris, J. L., Backes, B. J., Leonetti, F., Mahrus, S., Ellman, J. A., and Craik, C. S. (2000) *Proc. Natl. Acad. Sci. U.S.A. 97*, 7754−7759.
38. Backes, B. J., Harris, J. L., Leonetti, F., Craik, C. S., and Ellman, J. A. (2000) *Nat. Biotechnol. 18*, 187−193.
39. Maroux, S., and Desnuelle, P. (1969) *Biochim. Biophys. Acta 181*, 59−72.
40. Kaslik, G., Patthy, A., Balint, B., and Graf, L. (1995) *FEBS Lett. 370*, 179−183.
41. Varallyay, E., Pal, G., Patthy, A., Szilagyi, L., and Graf, L. (1998) *Biochem. Biophys. Res. Commun. 243*, 56−60.
42. Drinkwater, C. C., Evans, B. A., and Richards, R. I. (1987) *Biochemistry 26*, 6750−6756.
43. Blaber, M., Isackson, P. J., and Bradshaw, R. A. (1987) *Biochemistry 26*, 6742−6749.
44. Sahin-Toth, M., Graf, L., and Toth, M. (1999) *Biochem. Biophys. Res. Commun. 264*, 505−508.
45. Genain, C. P., Gritz, L., Joshi, N., Panicali, D., Davis, R. L., Whitaker, J. N., Letvin, N. L., and Hauser, S. L. (1997) *J. Neuroimmunol. 79*, 119−128.
46. Gardinier, M. V., Amiguet, P., Linington, C., and Matthieu, J.-M. (1992) *J. Neurosci. Res. 33*, 177−187.
47. Adelman, M., Wood, J., Benzel, I., Fiori, P., Lassmann, H., Matthieu, J.-M., Gardinier, M. V., Dornmair, K., and Linington, C. (1995) *J. Neuroimmunol. 63*, 17−27.
48. Amor, S., Groome, N., Linington, C., Morris, M. M., Dornmair, K., Gardinier, M. V., Matthieu, J.-M., and Baker, D. (1994) *J. Immunol. 153*, 4349−4356.
49. Bernard, C. C. A., Johns, T. G., Slavin, A., Ichikawa, M., Ewing, C., Liu, J., and Bettadapura, J. (1997) *J. Mol. Med. 75*, 77−88.

BI015781A